Supporting Information

Cation-Induced Strategy towards an Hourglass-Shaped $Cu_6I_7^-$ Cluster and its Color-Tunable Luminescence

Muxin Yu,[†,‡] Lian Chen,[†] Feilong Jiang,[†] Kang Zhou,[†] Caiping Liu,[†] Cai Sun,[†,‡] Xingjun Li,[†] Yan Yang,[†,‡] Maochun Hong*[†]*

[†]*State Key Laboratory of Structure Chemistry, Fujian Institute of Research on the Structure of Matter, Chinese Academy of Sciences, Fuzhou, China, 350002.*
[‡]*University of the Chinese Academy of Sciences, Beijing, China, 100049.*
[*]*Address correspondence to E-mail: cl@fjirsm.ac.cn; hmc@fjirsm.ac.cn*

Contents

Materials and methods

All chemicals and solvents used were purchased from commercial sources and used without further purification. The ligand tppa (tppa = N,N',N''-tris(3-pyridinyl)phosphoric triamide) was prepared according to the procedures outlined in the literature.[1] The Elemental analyses for C, H, and N were carried out on a Vario EL Ⅲ elemental analyzer, and inductively coupled plasma (ICP) spectroscopy was performed on an Ultima2 Inductively Coupled Plasma OES spectrometer. The powder X-ray diffraction (PXRD) patterns were collected by a RICAKU MiniFlex 600 diffractometer with Cu Kα radiation at room temperature with a step size of 0.01° in 2θ and a speed of 2°/min. The PXRD simulated pattern is based on single-crystal X-ray diffraction data using the Mercury Powder Pattern Calculate program.[2] Temperature-dependent X-ray diffraction experiments were performed on an Ultima-IV X-ray diffractometer with a step size of 0.01° in 2θ. Thermogravimetric analyses (TGA) were performed on a Netzsch STA 449C instrument from room temperature to 800 ºC with a heating rate of 10 ºC·min^{-1} under flowing nitrogen atmosphere. The IR spectra in the 400-4000 cm^{-1} region were collected with KBr pellets on a PerkinElmer Spectrum One FT-IR spectrometer. Photoluminescence spectra were investigated on a Horiba Jobin-Yvon Fluorolog-3 spectrophotometer analyzer and the overall fluorescence quantum yields were obtained on a calibrated integrating sphere at room temperature on Edinburgh Instruments FLS920 spectrofluorometer. Ball-milling experiment was carried on the Retsch MM400 at 30 Hz for 30 minutes.

Synthesis of $\{Li(H_2O)(EtOH)_3[Cu_6I_7(tppa)_2]\}_n$ (1-Li)

CuI (0.019 g, 0.1 mmol) and tppa (0.010 g, 0.03 mmol) were dissolved in 2 mL MeCN and 4 mL EtOH respectively, and then they were mixed on the addition of 0.8 mL LiI saturated aqueous solution. After filtration and evaporation under ambient conditions for 5 days, light yellow crystals were obtained in 35.0% yield based on the tppa ligand. Anal. Calcd (%) for $C_{36}H_{50}N_{12}O_6P_2LiCu_6I_7$ (Mr = 2085.36): C, 20.73; H, 2.42; N, 8.06; Li, 0.33; Cu, 18.28. Found (%): C, 21.09; H, 2.30; N, 8.20; Li, 0.32; Cu, 18.44. IR (KBr, main absorption bands): 3531(ν(O-H)), 3441(ν(-NH)), 3326(ν(O-H)), 3174 (ν(P=O)), 2972(ν(-CH_3)), 2843(ν(-CH_2)), 1580(ν(C=C)), 1467(ν(C=C)), 1272(ν(C-N)), 1193(ν(C-N)), 1050(ν(C-N)), 954(δ(Ar-H)), 789(δ(Ar-H)) and 693(δ(Ar-H)) cm^{-1}.

Synthesis of {$Na(H_2O)(EtOH)_3[Cu_6I_7(tppa)_2]$}$_n$ (1-Na)

The synthetic procedure was similar to that used in **1-Li** except LiI saturated aqueous solution was changed to NaI saturated aqueous solution. After filtration and evaporation, light yellow crystals were obtained in 53.4% yield based on the tppa ligand. Anal. Calcd (%) for $C_{36}H_{50}N_{12}O_6P_2NaCu_6I_7$ (Mr = 2101.40): C, 20.58; H, 2.40; N, 8.00; Na, 1.09; Cu, 18.14. Found (%): C, 20.92; H, 2.29; N, 8.26; Na, 1.11; Cu, 18.35. IR (KBr, main absorption bands): 3531(ν(O-H)), 3441(ν(-NH)), 3326(ν(O-H)), 3180 (ν(P=O)), 2972(ν($-CH_3$)), 2843(ν($-CH_2$)), 1580(ν(C=C)), 1467(ν(C=C)), 1272(ν(C-N)), 1193(ν(C-N)), 1050(ν(C-N)), 954(δ(Ar-H)), 789(δ(Ar-H)) and 695(δ(Ar-H)) cm^{-1}.

Synthesis of {$NH_4(H_2O)(EtOH)_3[Cu_6I_7(tppa)_2]$}$_n$ (1-NH_4)

NH_4I saturated aqueous solution was substituted for LiI saturated aqueous solution in synthetic progress of **1-Li** to obtain yellow crystals **1-NH_4** in 56.2% yield based on the tppa ligand. Anal. Calcd (%) for $C_{36}H_{54}N_{13}O_6P_2Cu_6I_7$ (Mr = 2096.45): C, 20.62; H, 2.60; N, 8.68; Cu, 18.19. Found (%): C, 20.29; H, 2.36; N, 8.96; Cu, 18.15. IR (KBr, main absorption bands): 3489(ν(O-H)), 3407(ν(-NH)), 3200(ν(P=O)), 2960(ν($-CH_3$)), 1580(ν(C=C)), 1465(ν(C=C)), 1380(ν(-CH3)), 1261(ν(C-N)), 1191(ν(C-N)), 1089(ν(-NH), 952(δ(Ar-H)), 800(δ(Ar-H)) and 696(δ(Ar-H)) cm^{-1}.

Synthesis of {$K(H_2O)_2(MeOH)_2[Cu_6I_7(tppa)_2]\cdot MeCN$}$_n$ (1-K)

A similar method to that of **1-Li** was employed, except EtOH and LiI saturated aqueous solution were replaced by MeOH and KI saturated aqueous solution addition respectively. After filtration and evaporation, yellow crystals were obtained. Yield: 45.3% based on the tppa ligand. Anal. Calcd (%) for $C_{34}H_{45}N_{13}O_6P_2KCu_6I_7$ (Mr = 2102.46): C, 19.42; H, 2.16; N, 8.66; K, 1.86; Cu, 18.13. Found (%): C, 19.63; H, 2.21; N, 8.52; K, 1.61; Cu, 18.31. IR (KBr, main absorption bands): 3483(ν(O-H)), 3558(ν(O-H)), 3400(ν(-NH)), 3180 (ν(P=O)), 2926(ν($-CH_3$)), 1580(ν(C=C)), 1468(ν(C=C)), 1272(ν(C-N)), 1193(ν(C-N)), 1050(ν(C-N)), 954(δ(Ar-H)), 789(δ(Ar-H)) and 693(δ(Ar-H)) cm^{-1}.

Synthesis of {$[N(Et)_4][Cu_6I_7(tppa)_2]$}$_n$ (1-TEA)

CuI (0.019 g, 0.1 mmol), tppa (0.010 g, 0.03 mmol) and tetraethylammonium iodide (TEAI) (0.1 g) were dissolved in a mixture of 2 mL MeCN and 5 mL EtOH, which then was placed in a glass vessel (15 mL) and heated at 85 ºC for 24 h. Bright yellow crystals of 1-TEA were obtained in 83.5% yield based on the tppa ligand. Anal. Calcd (%) for $C_{38}H_{50}N_{13}O_2P_2Cu_6I_7$ (Mr = 2052.44): C, 22.24; H, 2.46; N, 8.87; Cu, 18.58. Found (%): C, 22.59; H, 2.50; N, 8.99; Cu, 18.20. IR (KBr, main absorption bands): 3410(ν(-NH)), 3200(ν(P=O)), 2960(ν(-CH_3)), 2902(ν(-CH_2)), 1580(ν(C=C)), 1465(ν(C=C)), 1380(ν(-CH_3)), 1261(ν(C-N)), 1191(ν(C-N)), 1089(ν(C-N), 952(δ(Ar-H)), 800(δ(Ar-H)) and 696(δ(Ar-H)) cm^{-1}.

Synthesis of {[N(Pr)$_4$][Cu_6I_7(tppa)$_2$]}$_n$ (1-TPA)

CuI (0.019 g, 0.1 mmol), tppa (0.010 g, 0.03 mmol) and tetrapropylammonium iodide (TPAI) (0.55 g) were dissolved in a mixture of 2 mL MeCN and 5 mL EtOH. After filtration and evaporation under ambient conditions for 5 days, light yellow powders were obtained in 79.0% yield based on the tppa ligand. Anal. Calcd (%) for $C_{42}H_{58}N_{13}O_2P_2Cu_6I_7$ (Mr = 2108.55): C, 23.92; H, 2.77; N, 8.64; Cu, 18.08. Found (%): C, 23.96; H, 2.77; N, 8.48; Cu, 17.76. IR (KBr, main absorption bands): 3324(ν(-NH)), 3201(ν(P=O)), 3050(ν(-CH_3)), 2972(ν(-CH_2)), 1580(ν(C=C)), 1465(ν(C=C)), 1380(ν(-CH_3)), 1260(ν(C-N)), 1191(ν(C-N)), 1045(ν(C-N), 952(δ(Ar-H)), 800(δ(Ar-H)) and 694(δ(Ar-H)) cm^{-1}.

Synthesis of [Cu_2I_2(tppa)$_2$]$_n$ (2)

CuI (0.019 g, 0.1 mmol), tppa (0.010 g, 0.03 mmol) and tetrabutylammonium iodide (TBAI) (0.1 g) were dissolved in a mixture of 2 mL MeCN and 5 mL EtOH, which then was placed in a glass vessel (15 mL) and heated at 85 ºC for 24 h. Yellow crystals of **2** were obtained in 58.1% yield based on the tppa ligand. Anal. Calcd (%) for $C_{30}H_{30}N_{12}O_2P_2Cu_2I_2$ (Mr = 1033.49): C, 34.86; H, 2.92; N, 16.26; Cu, 12.30. Found (%): C, 34.75; H, 2.83; N, 16.06; Cu, 12.47. IR (KBr, main absorption bands): 3393(ν(-NH)), 3209(ν(P=O)), 3070(ν(Ar-H)), 1577(ν(C=C)), 1482(ν(C=C)), 1215(ν(C-N)), 1052(ν(C-N), 943(δ(Ar-H)), 805(δ(Ar-H)) and 702(δ(Ar-H)) cm^{-1}.

X-ray crystallography

Single-crystal X-ray diffraction data were collected on a Super Nova diffractometer equipped with a multilayer mirror Cu-Kα radiation (λ = 1.5418 Å) using a ω scan mode at 100 K. The structures were solved by direct methods and refined by full-matrix least-squares techniques on F^2 with SHELX-97.[3] Anisotropic refinement was performed to all non-hydrogen atoms except the tetraethylammonium cation in **1-TEA**. Hydrogen atoms from ligands were generated geometrically, while those on the solvent molecules could not be determined. The disordered solvents and NH_4 cation in **1-NH₄** were removed by the SQUEEZE process.[4] The final chemical formulas of the five compounds were calculated from solved results combined with TGA, elemental analysis, and ICP data. The CCDC numbers for **1-Li** to **1-TEA** and **2** are 1537508-1537512 and 1561914, respectively.

Structure and property description of compound 2

Single-crystal X-ray diffraction analyses reveal that the compound **2** crystallizes in *P*-1 space group, featuring a common neutral rhombohedral cluster Cu_2I_2. As Figure S1a shown, there are a ligand molecule, a Cu atom and an iodide atom in the asymmetric unit. Each Cu in the Cu_2I_2 motif is tetrahedrally coordinated to two μ_2-bridging I atoms and two N atoms from different ligands. The ligands serve as bidentate bridges connecting the neighboring Cu_2I_2 motifs to form a one-dimensional (1D) chain. The third pyridine of the tripodal ligand does not participate in coordination but hangs beside the chain (Figure S1b). These chains then close pack along the *a* and *b* axes as Figure S1c and Figure S1d shown. The phase purity of compound **2** was confirmed by the PXRD (Figure S2).

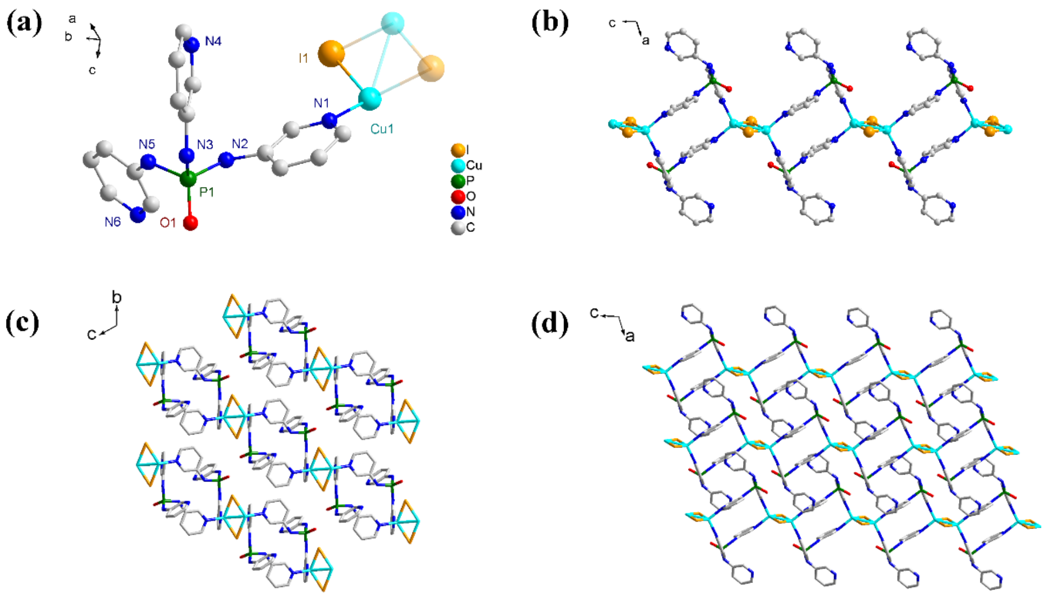

Figure S1. The structure presentation of **2**: (a) asymmetric unit; (b) 1D chain; (c) packing structure viewed along the *a* axis; (d) packing structure viewed along the *b* axis.

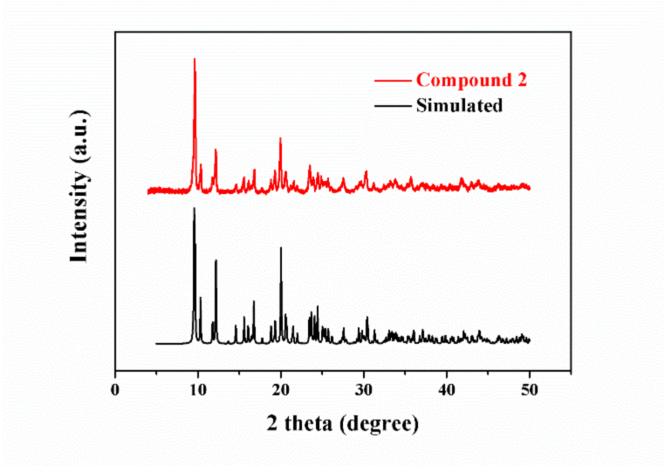

Figure S2. PXRD patterns of the compound **2**.

As Figure S3 shown, compound **2** exhibits an emission band with a maximum peak around 505 nm under excitation at 395 nm, which locates at (0.24, 0.47) in the CIE-1931chromaticity diagram. The QY of **2** is 4.4 ± 0.8%, and the lifetimes are 13.6 μs and 2.17 μs at 77 K and 298 K, respectively. The TGA analysis reveals that **2** decomposes at around 250 °C (Figure S4).

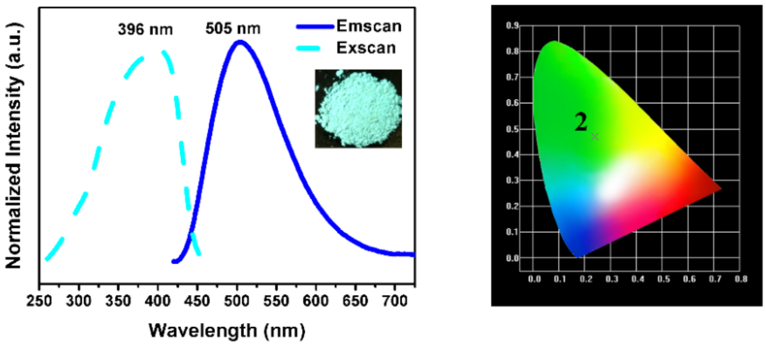

Figure S3. The photoluminescence spectra (left), powder sample under 365 nm UV light (insert) and CIE-1931 chromaticity diagram (right) of the compound **2**.

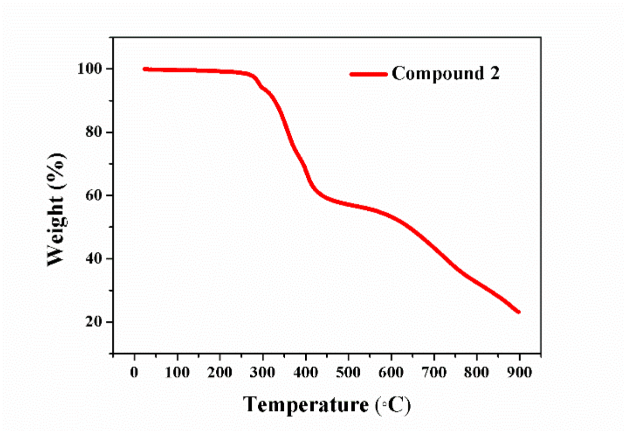

Figure S4. TG curve of compound **2**.

Computational Descriptions

The crystallographic data of the **1-Li**, **1-Na**, **1-NH$_4$**, **1-K**, and **1-TEA** were used to calculate their electronic densities of states. The calculations were performed with the CASTEP program and were based on density functional theory using a plane-wave basis set.[5] The exchange-correlation energy was calculated using the Perdew-Burke-Ernzerhof modification to the generalized gradient approximation.[6] The norm-conserving and ultrasoft pseudopotentials were chosen to modulate the electron-ion interaction for compounds **1-Li** to **1-K** and **1-TEA**, respectively.[7] The orbital electrons of C $2s^22p^2$, H $1s^1$, N $2s^22p^3$, O $2s^22p^4$, P $3s^23p^3$, I $5s^25p^5$, Li $2s^1$, Na $2s^22p^63s^1$, K $3s^23p^64s^1$ and Cu $3d^{10}4s^2$ were treated as valence electrons. The number of plane waves included in the basis was determined by a cutoff energy of 800 eV and 240 eV for compounds **1-Li** to **1-K** and **1-TEA**, respectively. The numerical integration of the Brillouin zone was performed by using 1 × 1 × 1 Monkhorst Pack *k*-point sampling for all compounds. Other parameters used in the calculations were set by the default values of the CASTEP code.

LEDs fabrication and performance measurement

Two-component white LEDs of different contents of **1-TEA** were fabricated by combining UV chips (380 nm, 1W, 350 mA, Epileds), BAM:Eu^{2+} blue phosphor and **1-TEA** yellow phosphor. The two-component phosphors were mixed with silicone thoroughly and the obtained phosphor-silicone mixture was coated on the surface of the LED chips to produce LEDs. The photoelectric properties of the fabricated devices were measured by an integrating sphere spectroradiometer system (LHS-1000, Everfine). The LEDs were operated at 3.0 V with drive currents of 350 mA. The spectral power distributions of the LEDs were measured by a corrected spectrometer to calculate their values of CCT and CRI.[8] The current density−voltage−brightness (I−V−B) curves of the devices were recorded on a Keithley 2400/2000 source meter and a calibrated silicon photodiode. All measurements on the devices were carried out at room temperature.

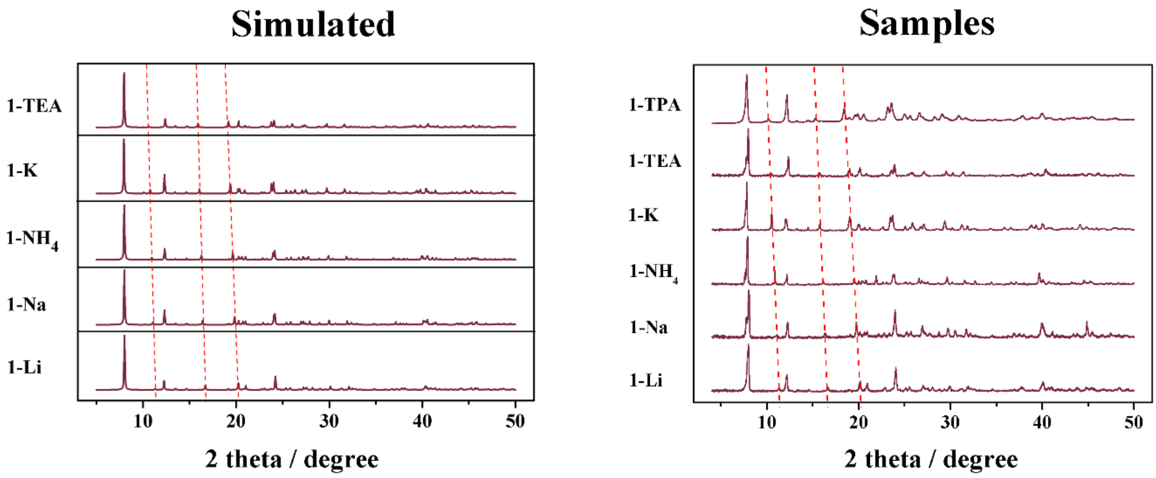

Figure S5. PXRD patterns of the compounds **1-Li**, **1-Na**, **1-NH$_4$**, **1-K**, **1-TEA**, and **1-TPA**.

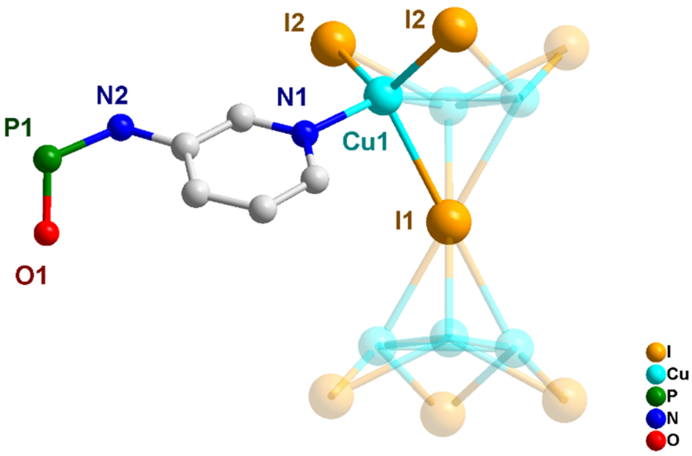

Figure S6. The coordination environment of the Cu(I) in the $Cu_6I_7^-$ cluster.

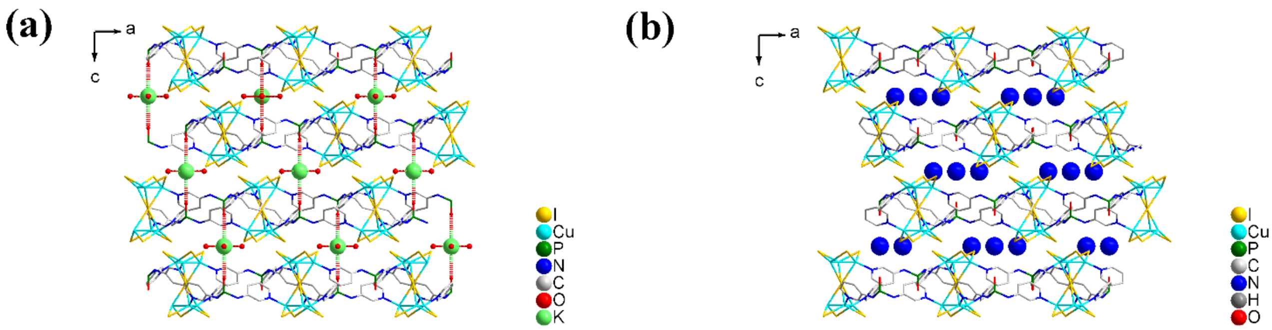

Figure S7. (a) Real structure model of the complexes with alkali metal cations (**1-K** as a representative). (b) Real structure model of the complexes with ammonium cations (**1-NH$_4$** as a representative).

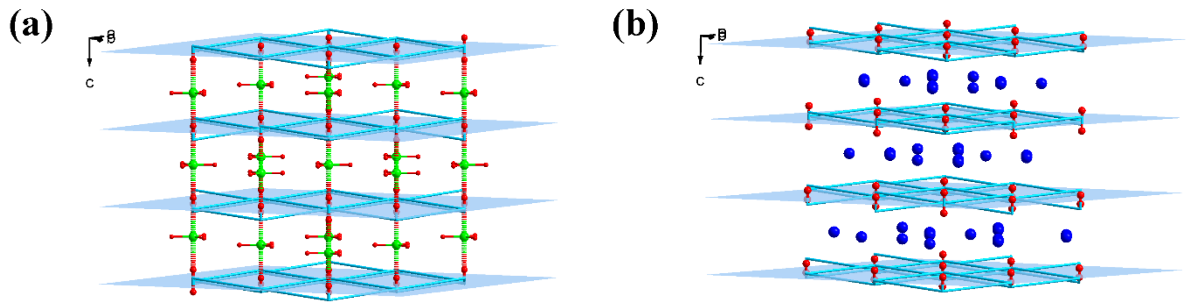

Figure S8. (a) Illustration of interlamellar structure in the complexes with alkali metal cations (**1-K** as a representative). (b) Illustration of interlamellar structure in the complexes with ammonium cations (**1-NH$_4$** as a representative). Color scheme of the balls: K^+, green; NH_4^+, blue; O, red; layer, cyan. Ligands and clusters are omitted for clarity.

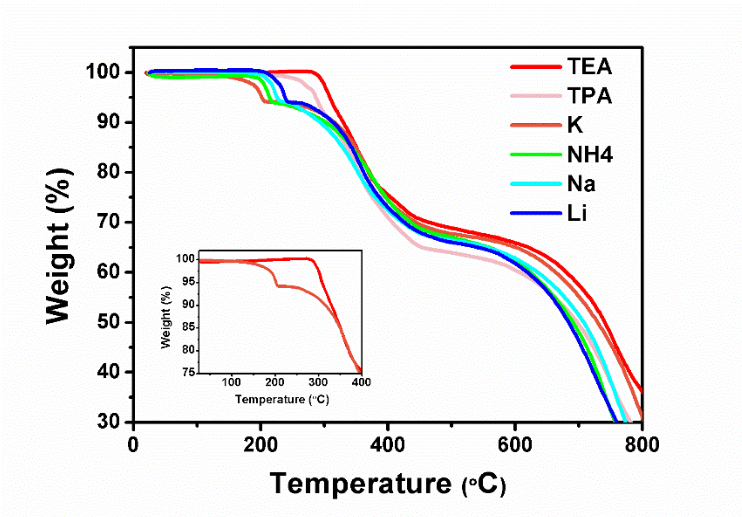

Figure S9. TG curves of the six compounds. Inner: the amplification of **1-K** and **1-TEA** curves.

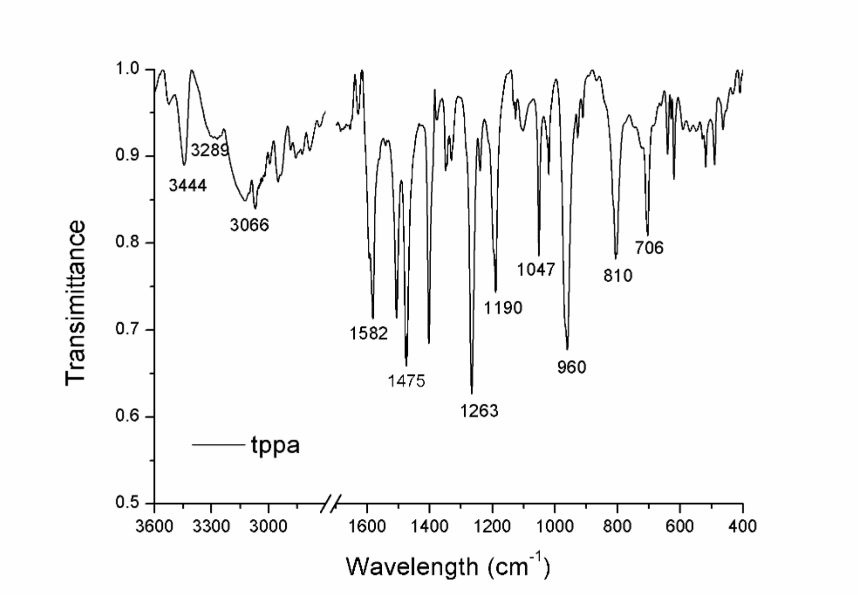

Figure S10. FT-IR spectrum of the ligand (tppa) with labeled main peaks.

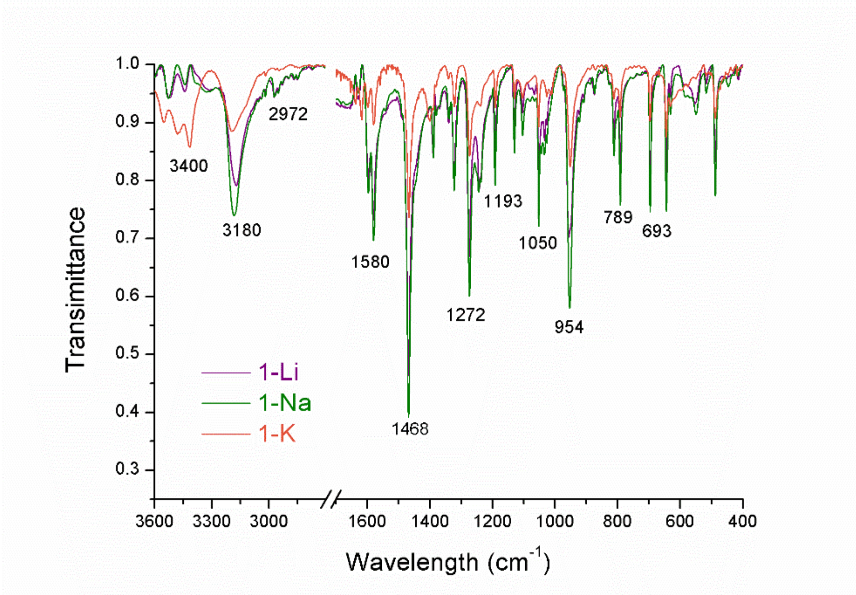

Figure S11. FT-IR spectra of the compounds **1-Li**, **1-Na**, and **1-K** with labeled main peaks.

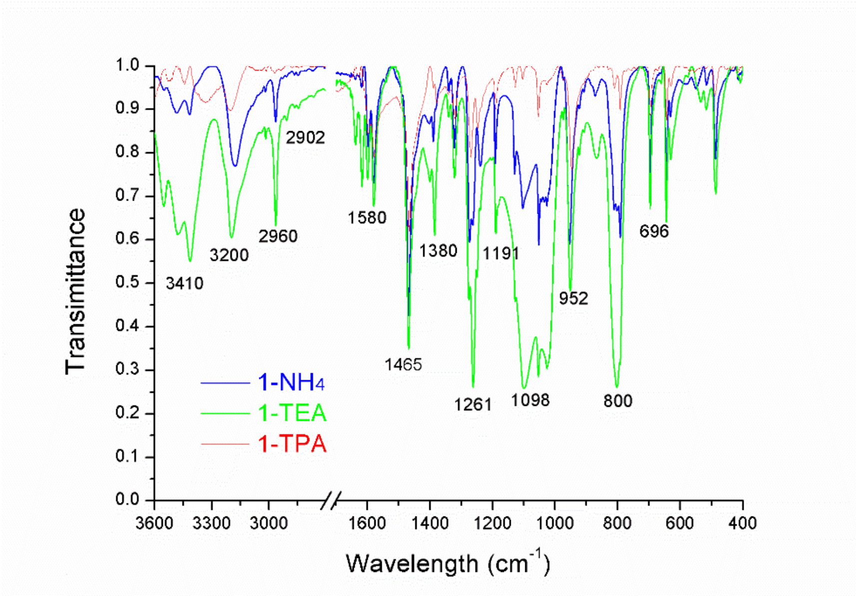

Figure S12. FT-IR spectra of the compounds **1-NH$_4$**, **1-TEA**, and **1-TPA** with labeled main peaks.

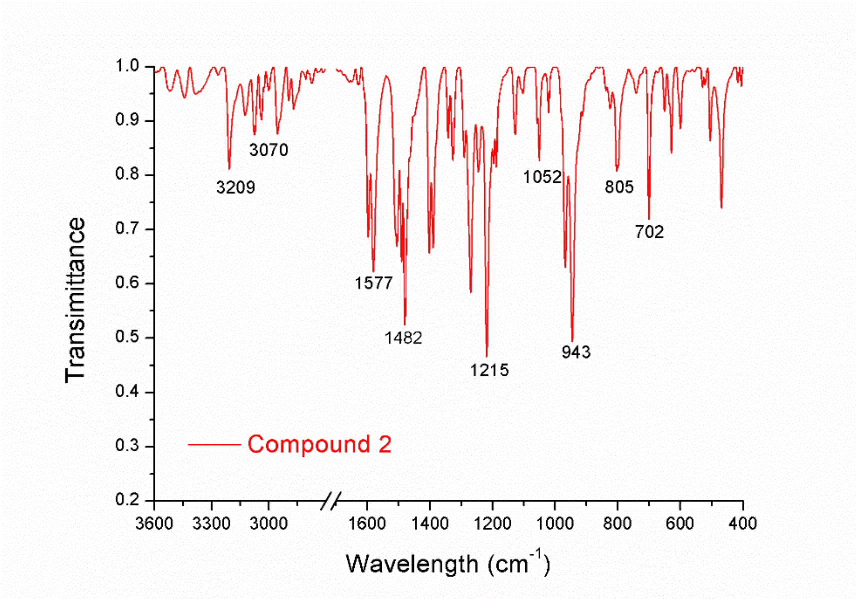

Figure S13. FT-IR spectrum of the compound **2** with labeled main peaks.

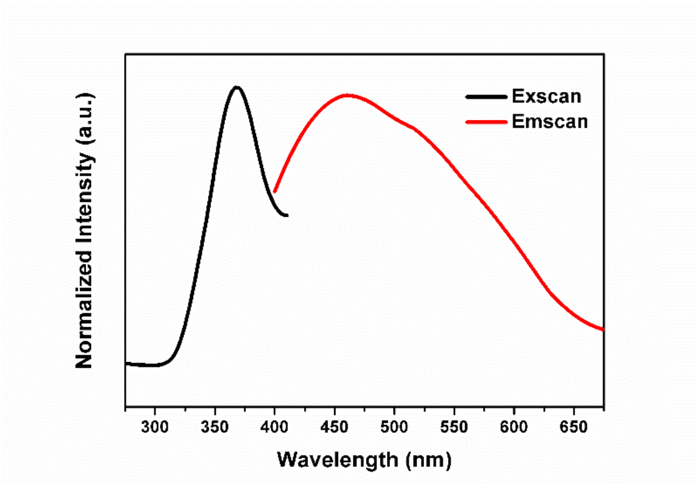

Figure S14. The excitation (black) and emission (red) spectra of the ligand (tppa).

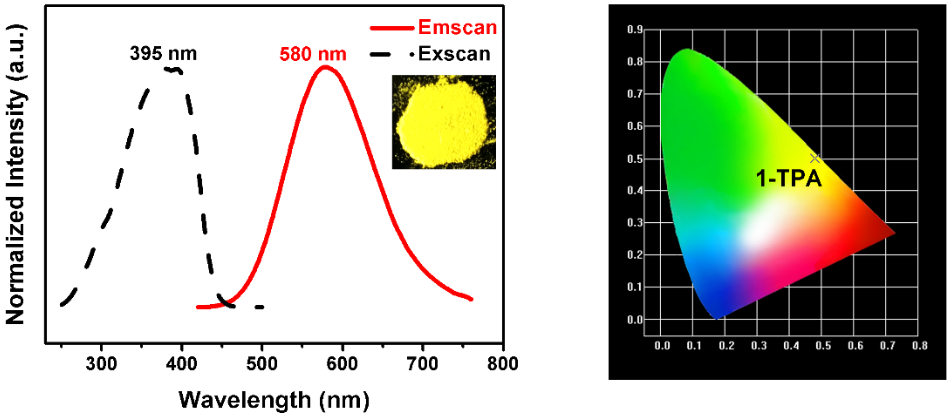

Figure S15. The photoluminescence spectra (left), powder sample under 365 nm UV light (insert) and CIE-1931 chromaticity diagram (right) of the compound **1-TPA**.

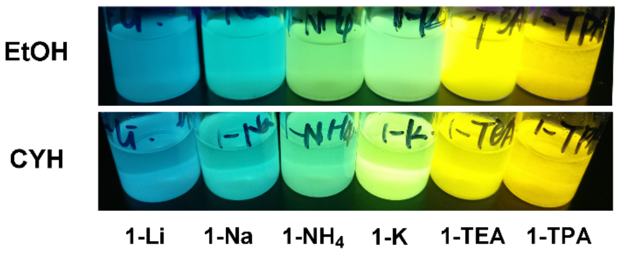

Figure S16. Photoluminescence images of the six compounds dispersing in EtOH (upper) and cyclohexane (nether) under the 365 nm UV light.

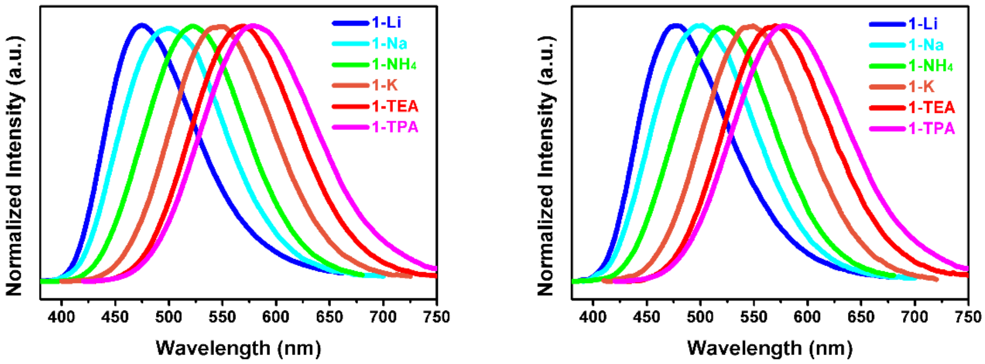

Figure S17. The emission spectra of the six compounds dispersing in EtOH (left) and cyclohexane (right).

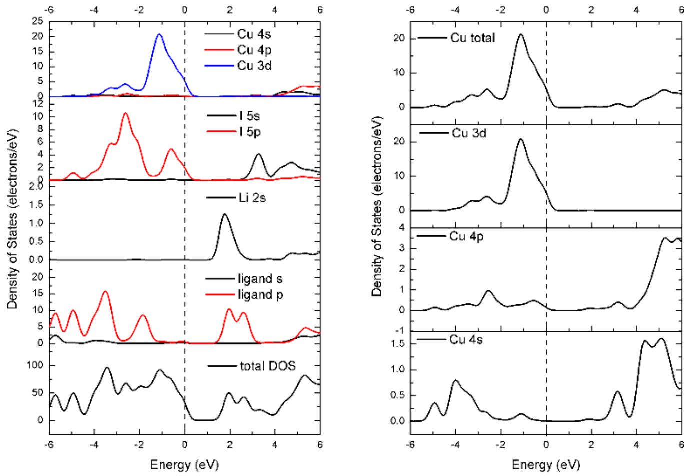

Figure S18. Calculated DOS for **1-Li**: total and partial DOS (left); Cu partial DOS (right).

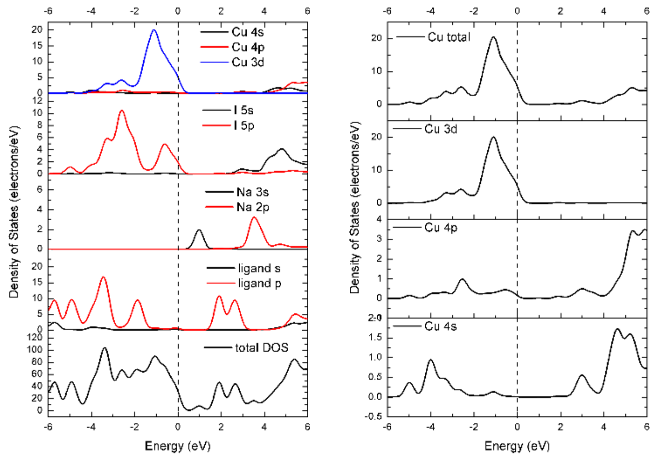

Figure S19. Calculated DOS for **1-Na**: total and partial DOS (left); Cu partial DOS (right).

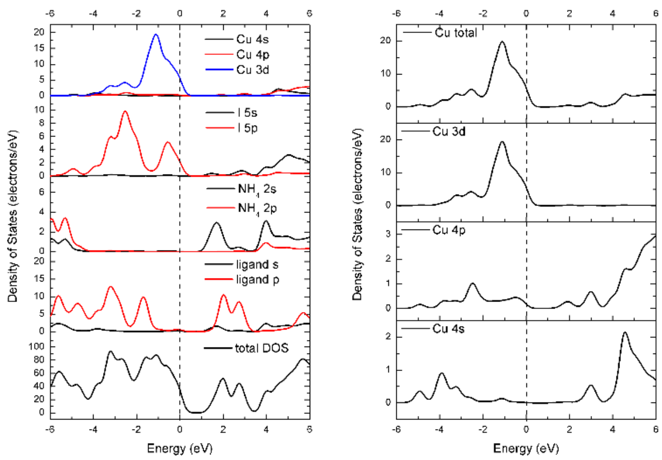

Figure S20. Calculated DOS for **1-NH$_4$**: total and partial DOS (left); Cu partial DOS (right).

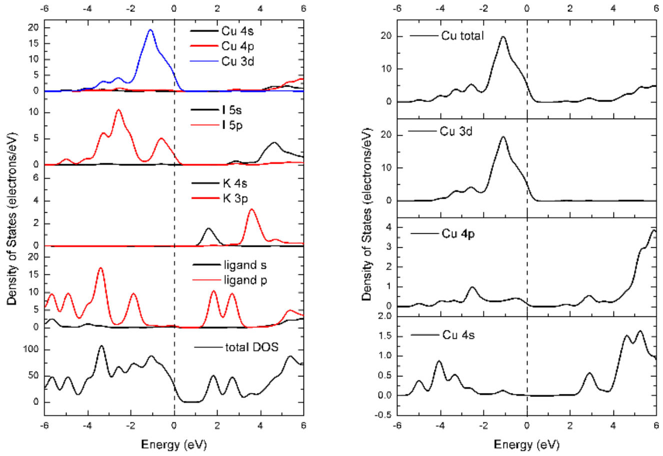

Figure S21. Calculated DOS for **1-K**: total and partial DOS (left); Cu partial DOS (right).

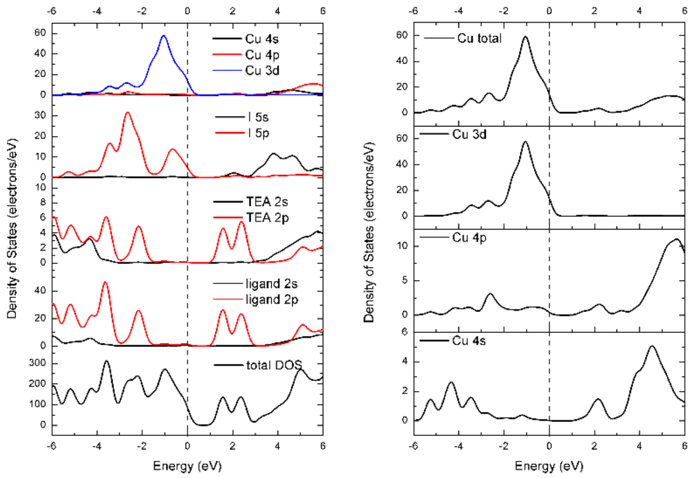

Figure S22. Calculated DOS for **1-TEA**: total and partial DOS (left); Cu partial DOS (right).

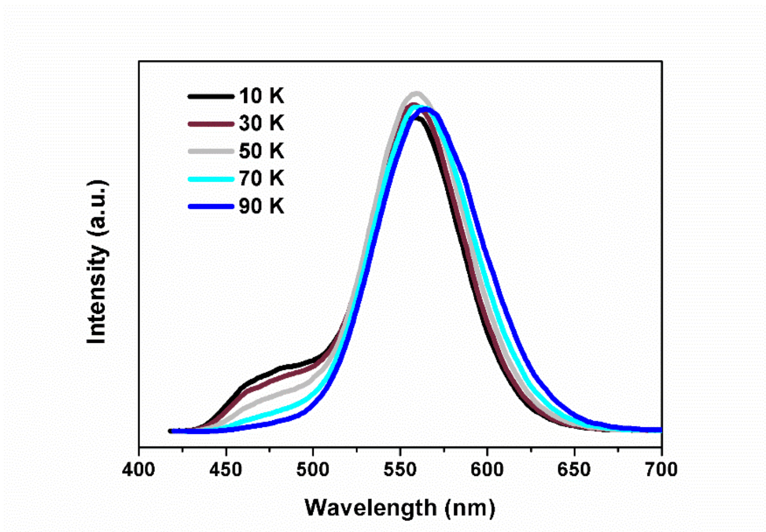

Figure S23. Luminescence spectra of **1-K** excited at 375 nm at low temperature.

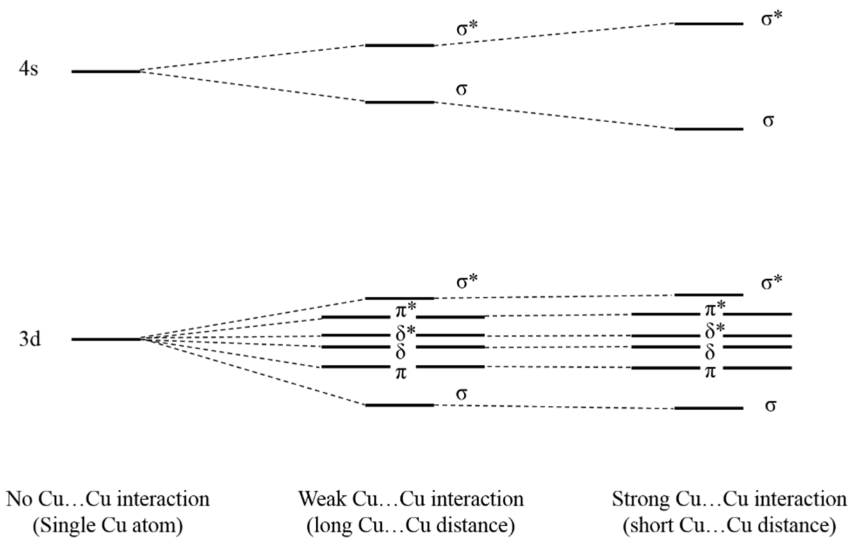

Scheme S1. A schematic representation of the relationship between the Cu…Cu interactions and the splittings of the frontier metal orbitals (3d → 4s as a representative).

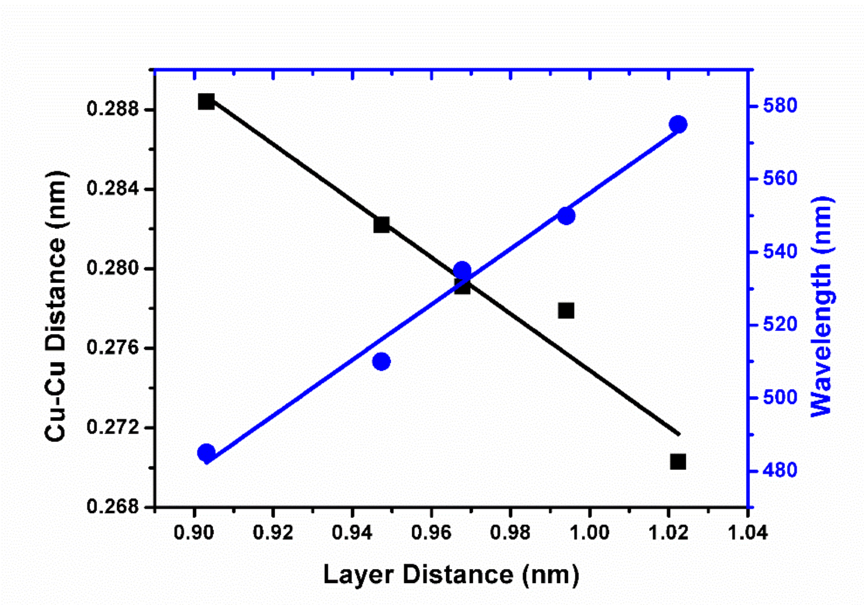

Scheme S2. Relationship of the Cu-Cu distance (left, black) and the emission wavelength (right, blue) with the layer distance of the five compounds. The linear fits show Equations y = -0.142 x + 0.417, R^2 = 0.0.947 (left, black) and y = 762 x - 206, R^2 = 0.983 (right, blue).

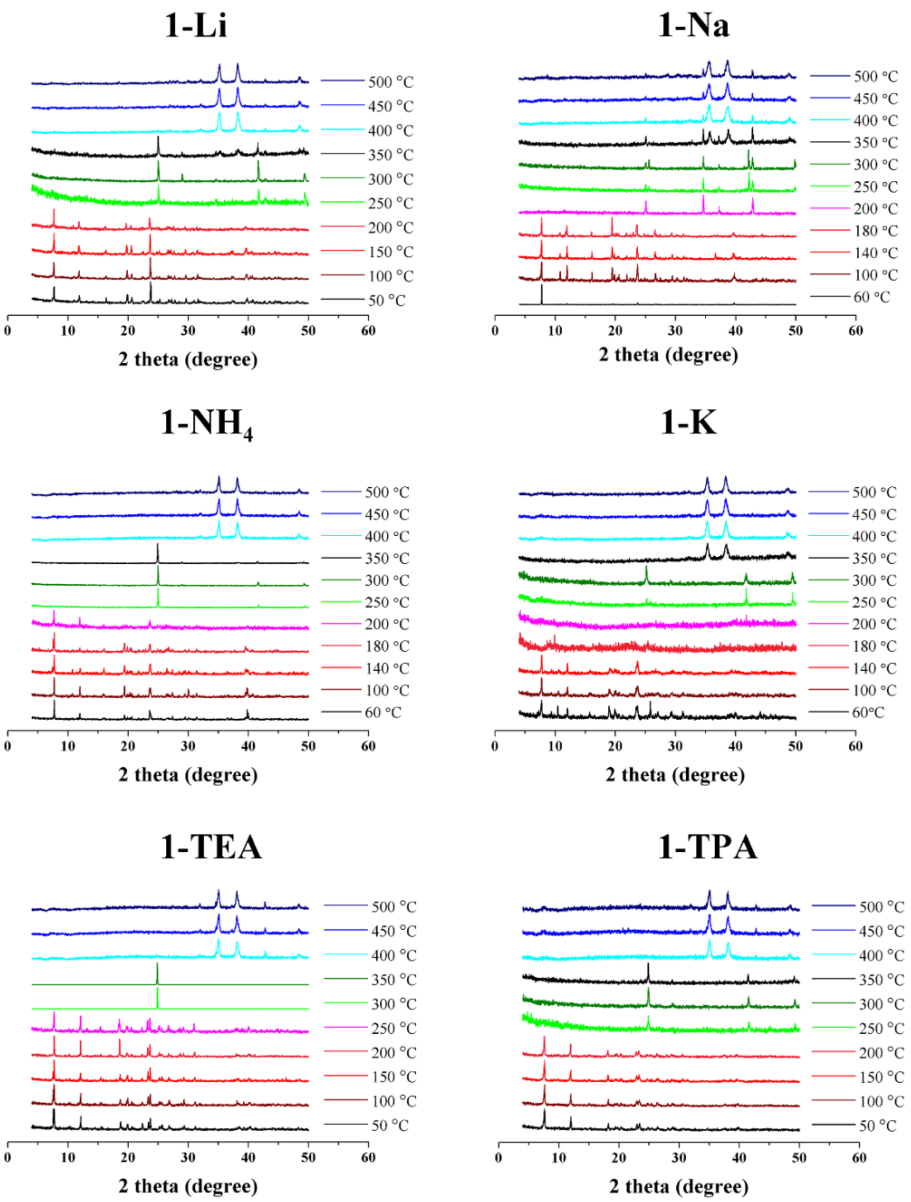

Figure S24. TD-PXRD patterns of the compounds **1-Li**, **1-Na**, **1-NH$_4$**, **1-K**, **1-TEA**, and **1-TPA**.

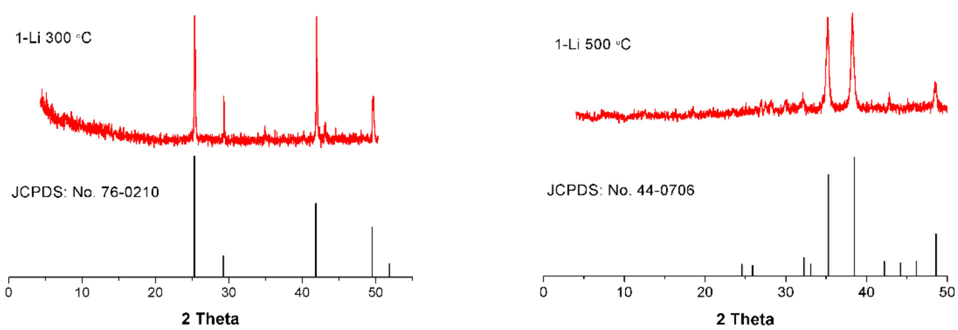

Figure S25. PXRD patterns of **1-Li** at 300 ºC (left) in accordance with CuI structure (JCPDS: No. 76-0210) and at 500 ºC in accordance with CuO structure (JCPDS: No. 44-0706) (right).

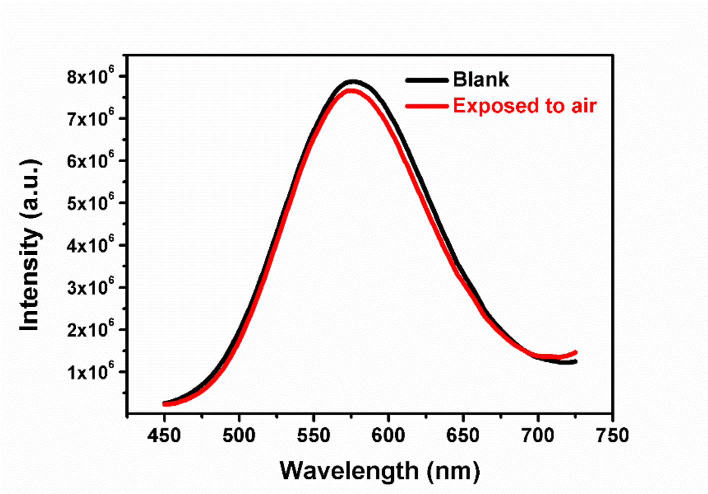

Figure S26. PL intensity of **1-TEA** after exposed to open air for six months (red) and freshly prepared (black).

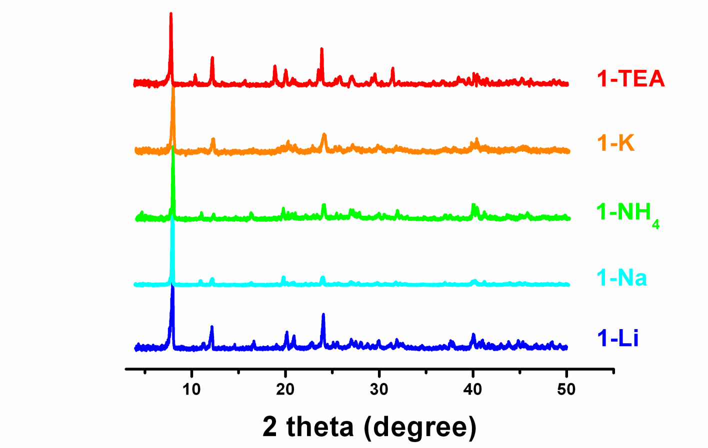

Figure S27. PXRD patterns of the five compounds after heating at 120 ºC for 48 h.

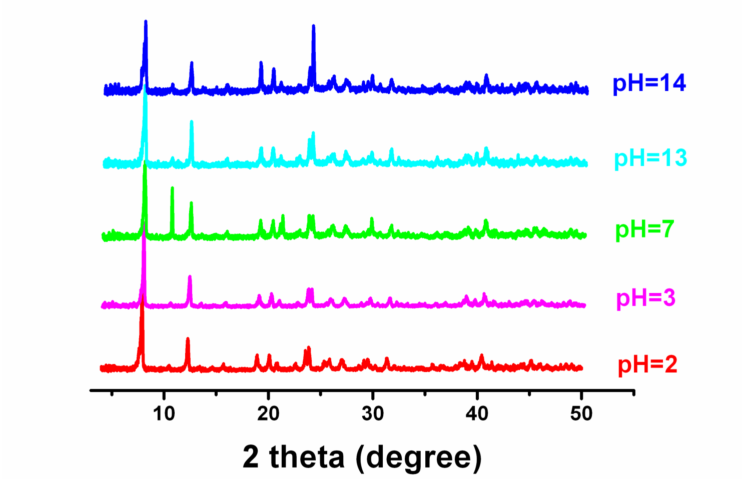

Figure S28. PXRD patterns of **1-TEA** after immersing in pH 2-14 buffer solutions for 24 h.

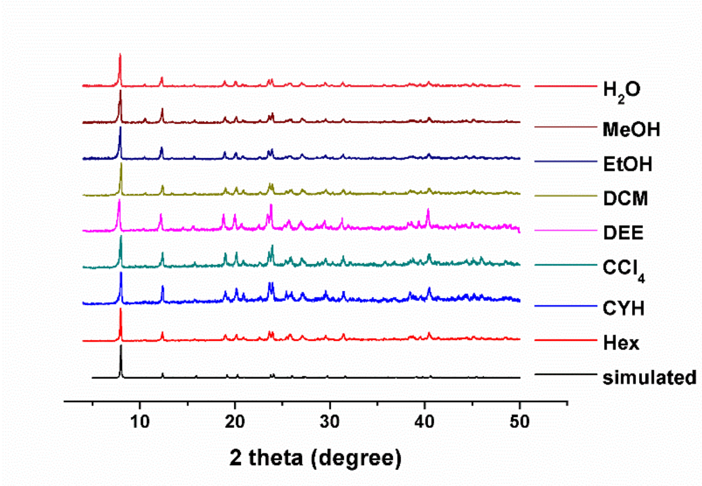

Figure S29. PXRD patterns of **1-TEA** after soaking in water (H_2O), methanol (MeOH), ethanol (EtOH), dichloromethane (DCM), diethyl ether (DEE), tetrachloromethane (CCl_4), cyclohexane (CYH) and hexane (Hex) solvents for 35 days.

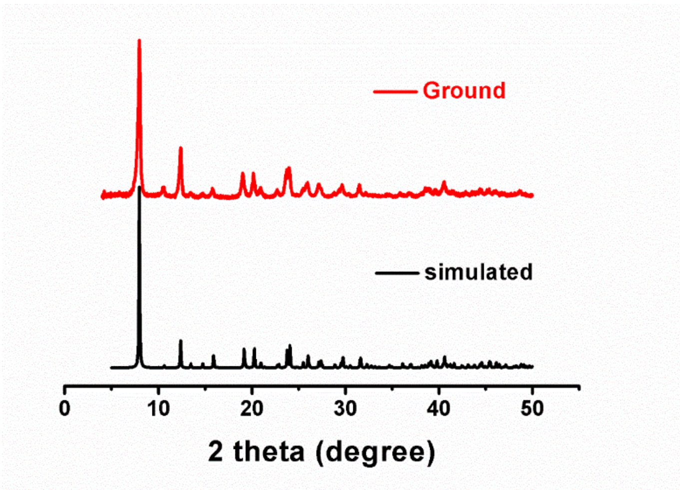

Figure S30. PXRD patterns of **1-TEA** after ball milling at 30 Hz for 30 min.

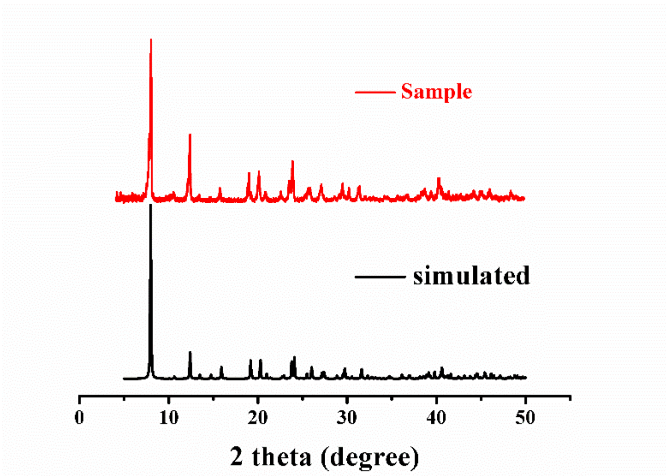

Figure S31. PXRD patterns of **1-TEA** after exposed to open air for six months.

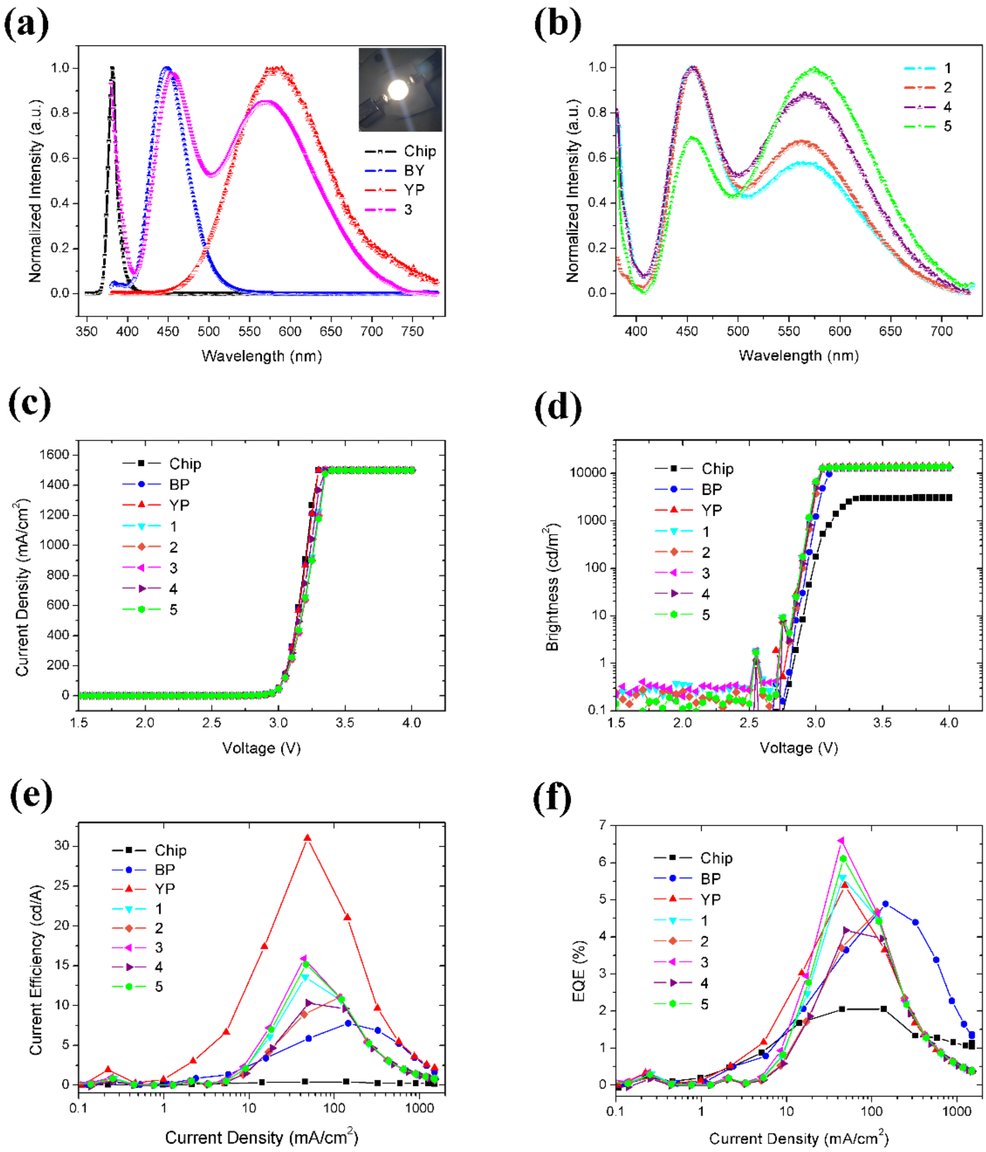

Figure S32. (a) EL spectra of the chip, **BP** (BAM: Eu^{2+}), **YP** (**1-TEA**), and the **3** LEDs. Inset: lighted LED of **3**. (b) EL spectra of **1**, **2**, **4**, and **5** LEDs. Current density-voltage (I-V) curves (c), brightness-voltage (B-V) curves (d), plots of current efficiency vs current density (e) and plots of external quantum efficiency vs current density (f) for the LEDs.

Table S1. Important photoelectric parameters for LEDs **1-5.**

Device	YP amount (wt%)	V_{on} (V)	B_{max} (cd/m^2)	CE_{max} (cd/A)	EQE_{max} (%)	CIE	CRI	CCT
Chip	-	2.85	3166	0.4	2.1	0.1900, 0.0787	-	-
BP	0	2.85	13770	6.8	4.9	0.1453, 0.0614	-	-
YP	100	2.70	14205	31.0	5.4	0.4748 0.4941	-	-
1	1.7	2.75	13178	9.1	4.2	0.2881, 0.2933	86.5	8950
2	2.6	2.75	13514	11.0	4.7	0.2960, 0.3136	81.6	7744
3	4.1	2.70	13422	15.9	6.6	0.3261, 0.3345	83.8	5850
4	7.5	2.75	13441	10.3	4.2	0.3243, 0.3469	79.7	5794
5	8.0	2.75	13931	15.2	6.1	0.3592, 0.3819	76.1	4628

Table S2. Crystal data and refinement results for **1-Li**, **1-Na**, **1-NH$_4$**, **1-K**, **1-TEA**, and **2**.

Compound	**1-Li**	**1-Na**	**1-NH$_4$**
Formula	$C_{36}H_{50}N_{12}O_6P_2LiCu_6I_7$	$C_{36}H_{50}N_{12}O_6P_2NaCu_6I_7$	$C_{36}H_{54}N_{13}O_6P_2Cu_6I_7$
Formula weight	2085.36	2101.40	2096.45
Crystal system	trigonal	trigonal	trigonal
space group	*R*-3*c*	*R*-3*c*	*R*-3*c*
a/*b* (Å)	14.4114 (5)	14.3640(2)	14.3430(2)
c (Å)	46.858 (2)	47.9353(8)	48.4451(9)
α/*β*(°)	90°	90°	90°
γ (°)	120°	120°	120°
Volume (Å^3)	8428.0 (7)	8565.2(3)	8631.0(3)
T (K)	100	100	100
Z	6	6	6
F (000)	5616	5520	5310
R_1 (I>2σ(I))	0.0442	0.0341	0.0335
wR_2 (reflections)	0.1226	0.0984	0.1128
Goodness of fit on F^2	1.050	1.090	1.125
Compound	**1-K**	**1-TEA**	**2**
Formula	$C_{34}H_{45}N_{13}O_6P_2KCu_6I_7$	$C_{38}H_{50}N_{13}O_2P_2Cu_6I_7$	$C_{15}H_{15}N_6OPCuI$
Formula weight	2102.46	2052.44	899.06
Crystal system	trigonal	trigonal	triclinic
space group	*R*-3*c*	*R*-3*c*	*P*-1
a (Å)	14.3646(8)	14.2783(4)	9.0437(6)
b (Å)	14.3646(8)	14.2783(4)	10.8072(6)
c (Å)	49.201(3)	49.8573(14)	10.8381(7)
α (°)	90°	90°	116.350(6)°
β(°)	90°	90°	102.549(6) °
γ (°)	120°	120°	96.607(5)°
Volume (Å3)	8792.1(13)	8802.6(6)	899.06(12)
T (K)	100	100	100
Z	6	6	2
F (000)	5424	5640	504.0
R1 (I>2σ(I))	0.0471	0.0358	0.0315
wR2 (reflections)	0.1413	0.1055	0.0819
Goodness of fit on F2	1.104	1.241	1.055

Table S3. Selected bond lengths (Å) and bond angles (°) for **1-Li**, **1-Na**, **1-NH$_4$**, **1-K**, and **1-TEA**.

	1-Li	**1-Na**	**1-NH$_4$**	**1-K**	**1-TEA**
I1—Cu1^{i}	2.8424 (12)	2.8425 (9)	2.8430 (5)	2.8501 (13)	2.8728 (10)
I1—Cu1^{ii}	2.8426 (12)	2.8425 (9)	2.8431 (5)	2.8501 (13)	2.8728 (10)
I1—Cu1	2.8426 (11)	2.8425 (9)	2.8431 (5)	2.8501 (13)	2.8728 (10)
I1—Cu1^{iii}	2.8426 (11)	2.8425 (9)	2.8431 (5)	2.8502 (13)	2.8728 (10)
I1—Cu1^{iv}	2.8426 (11)	2.8426 (9)	2.8431 (5)	2.8501 (13)	2.8728 (10)
I1—Cu1^{v}	2.8426 (11)	2.8426 (9)	2.8431 (5)	2.8502 (13)	2.8728 (10)
I2—Cu1	2.5903 (12)	2.5898 (10)	2.5916 (5)	2.5933 (14)	2.5998 (11)
I2—Cu1^{ii}	2.5919 (12)	2.5958 (10)	2.5969 (5)	2.5948 (14)	2.6038 (11)
Cu1—N1	2.059 (6)	2.062 (5)	2.060 (2)	2.049 (8)	2.050 (6)
Cu1—I2^{i}	2.5904 (12)	2.5898 (9)	2.5916 (5)	2.5947 (14)	2.5998 (10)
Cu1—Cu1^{i}	2.8843 (19)	2.8215 (16)	2.7917 (7)	2.779 (2)	2.7031 (17)
Cu1—Cu1^{ii}	2.8843 (19)	2.8216 (16)	2.7917 (7)	2.779 (2)	2.7031 (17)
Cu1^{i}—I1—Cu1^{ii}	60.97 (4)	59.51 (3)	58.809 (14)	58.36 (4)	56.13 (3)
Cu1^{i}—I1—Cu1	60.97 (4)	59.51 (3)	58.809 (14)	58.36 (4)	56.13 (3)
Cu1^{ii}—I1—Cu1	60.97 (4)	59.51 (3)	58.809 (14)	58.36 (4)	56.13 (3)
Cu1^{i}—I1—Cu1^{iii}	180.0	180.00 (2)	180.000 (10)	180.0	180.0
Cu1^{ii}—I1—Cu1^{iii}	119.03 (4)	120.49 (3)	121.191 (14)	121.64 (4)	123.87 (3)
Cu1—I1—Cu1^{iii}	119.03 (4)	120.49 (3)	121.191 (14)	121.64 (4)	123.87 (3)
Cu1^{i}—I1—Cu1^{iv}	119.03 (4)	120.49 (3)	121.191 (14)	121.64 (4)	123.87 (3)
Cu1^{ii}—I1—Cu1^{iv}	119.03 (4)	120.49 (3)	121.191 (14)	121.64 (4)	123.87 (3)
Cu1—I1—Cu1^{iv}	180.00 (3)	180.0	180.0	180.0	180.00 (2)
Cu1^{iii}—I1—Cu1^{iv}	60.97 (4)	59.51 (3)	58.809 (14)	58.36 (4)	56.13 (3)
Cu1^{i}—I1—Cu1^{v}	119.03 (4)	120.49 (3)	121.191 (14)	121.64 (4)	123.87 (3)
Cu1^{ii}—I1—Cu1^{v}	180.0	180.00 (2)	180.0	180.00 (3)	180.00 (2)
Cu1—I1—Cu1^{v}	119.03 (4)	120.49 (3)	121.191 (14)	121.64 (4)	123.87 (3)
Cu1^{iii}—I1—Cu1^{v}	60.97 (4)	59.51 (3)	58.809 (14)	58.36 (4)	56.13 (3)

Cu1^{iv}—I1—Cu1^{v}	60.97 (4)	59.51 (3)	58.809 (14)	58.36 (4)	56.13 (3)
Cu1—I2—Cu1^{ii}	67.64 (5)	65.93 (4)	65.10 (2)	64.78 (6)	62.59 (5)
N1—Cu1—I2	108.99 (17)	107.93 (14)	107.63 (7)	107.6 (2)	108.01 (16)
N1—Cu1—I2^{i}	105.92 (17)	105.86 (14)	105.47 (7)	106.1 (2)	103.37 (16)
I2—Cu1—I2^{i}	125.97 (5)	125.26 (4)	125.045 (19)	123.68 (6)	125.00 (4)
N1—Cu1—Cu1^{i}	143.06 (17)	142.75 (14)	141.14 (7)	141.4 (2)	139.76 (16)
I2—Cu1—Cu1^{i}	109.55 (4)	110.20 (3)	110.355 (16)	110.26 (5)	111.50 (4)
I2^{i}—Cu1—Cu1^{i}	56.15 (4)	56.93 (4)	57.539 (17)	57.58 (5)	58.78 (4)
N1—Cu1—Cu1^{ii}	143.06 (17)	141.07 (14)	142.92 (7)	142.7 (2)	143.72 (16)
I2—Cu1—Cu1^{ii}	56.15 (4)	57.14 (3)	57.357 (17)	57.63 (5)	58.63 (4)
I2^{i}—Cu1—Cu1^{ii}	109.55 (4)	110.03 (3)	110.513 (15)	110.22 (4)	111.63 (4)
Cu1^{i}—Cu1—Cu1^{ii}	60.0	60.0	60.0	60.000 (1)	60.0
N1—Cu1—I1	100.93 (17)	100.32 (14)	100.08 (7)	99.8 (2)	97.99 (15)
I2—Cu1—I1	106.16 (4)	107.45 (3)	107.982 (15)	108.55 (5)	109.51 (4)
I2^{i}—Cu1—I1	106.12 (4)	107.28 (3)	107.833 (16)	108.50 (5)	109.39 (3)
Cu1^{i}—Cu1—I1	59.515 (17)	60.244 (14)	60.597 (7)	60.82 (2)	61.935 (16)
Cu1^{ii}—Cu1—I1	59.515 (18)	60.245 (14)	60.596 (7)	60.82 (2)	61.935 (16)

Symmetry codes: (i) 1-x+y, 2-x, z; (ii) 2-y, 1+x-y, z; (iii) -y, 1+x-y, z; (iv) x, 2+y, 2+z; (v) 2-y, x-y, 1+z; (vi) 1-y, 1+x-y, z; (vii) -x+y, 1-x, z; (viii) x, y, 1+z.

Table S4. Selected bond lengths (Å) and bond angles (°) for compound **2.**

Atom	Atom	Length/Å	Atom	Atom	Length/Å
I1	Cu1	2.6145(6)	N6	C17	1.342(5)
I1	Cu1^{1}	2.6338(6)	N6	C21	1.332(5)
Cu1	I1^{1}	2.6338(6)	N4	C16	1.340(5)
Cu1	Cu1^{1}	2.6355(10)	N4	C13	1.337(5)
Cu1	N1	2.061(3)	C12	C14	1.398(5)
Cu1	N6^{2}	2.068(3)	C12	C13	1.394(5)
P1	O1	1.478(3)	C18	C17	1.404(5)
P1	N2	1.661(3)	C18	C19	1.394(6)
P1	N5	1.650(4)	C11	C10	1.380(6)

P1	N3	1.644(3)	C8	C7	1.395(5)
N1	C11	1.346(5)	C8	C9	1.394(5)
N1	C7	1.339(5)	C16	C15	1.390(6)
N2	C8	1.395(5)	C15	C14	1.389(5)
N5	C18	1.399(5)	C19	C20	1.381(5)
N3	C12	1.402(4)	C9	C10	1.384(7)
N6	Cu1^{2}	2.068(3)	C20	C21	1.393(5)

Atom	**Atom**	**Atom**	**Angle/°**	**Atom**	**Atom**	**Atom**	**Angle/°**
Cu1	I1	Cu1^{1}	60.28(2)	C21	N6	Cu1^{2}	119.2(2)
I1	Cu1	I1^{1}	119.72(2)	C21	N6	C17	118.8(3)
I1^{1}	Cu1	Cu1^{1}	59.50(2)	C13	N4	C16	118.3(3)
I1	Cu1	Cu1^{1}	60.22(2)	C14	C12	N3	119.1(3)
N1	Cu1	I1^{1}	106.76(9)	C13	C12	N3	123.0(3)
N1	Cu1	I1	109.37(10)	C13	C12	C14	117.9(3)
N1	Cu1	Cu1^{1}	128.11(8)	N5	C18	C17	121.5(3)
N1	Cu1	N6^{2}	103.91(12)	C19	C18	N5	120.0(3)
N6^{2}	Cu1	I1	108.60(9)	C19	C18	C17	118.5(3)
N6^{2}	Cu1	I1^{1}	107.36(10)	N1	C11	C10	121.9(4)
N6^{2}	Cu1	Cu1^{1}	127.92(9)	N2	C8	C7	118.8(3)
O1	P1	N2	114.23(16)	C9	C8	N2	123.7(3)
O1	P1	N5	116.65(17)	C9	C8	C7	117.4(4)
O1	P1	N3	109.46(15)	N6	C17	C18	122.1(4)
N5	P1	N2	102.16(16)	N4	C16	C15	122.0(3)
N3	P1	N2	108.82(16)	N1	C7	C8	123.6(3)
N3	P1	N5	104.83(16)	C14	C15	C16	119.9(3)
C11	N1	Cu1	120.0(3)	C20	C19	C18	118.8(3)
C7	N1	Cu1	120.4(2)	C10	C9	C8	118.9(4)
C7	N1	C11	118.1(3)	C15	C14	C12	118.3(3)
C8	N2	P1	126.0(3)	N4	C13	C12	123.7(3)
C18	N5	P1	129.1(3)	C19	C20	C21	119.2(4)
C12	N3	P1	129.0(3)	C11	C10	C9	119.9(4)
C17	N6	Cu1^{2}	121.8(3)	N6	C21	C20	122.6(4)

Symmetry codes: (1) -X,-Y,-Z; (2) -X,1-Y,1-Z

References:

1. Li, N.; Jiang, F.; Chen, L.; Li, X.; Chen, Q.; Hong, M. From discrete octahedral nanocages to 1D coordination polymer: coordination-driven a single-crystal-to-single-crystal transformation via anion exchange. *Chem. Commun.* **2011**, *47*, 2327-2329.
2. http://www.ccdc.cam.au.uk/mercury/
3. Sheldrick, G. M. *SHELX-97: Programs for crystal structure analysis.* Göttingen, Germany (1997).
4. Vandersluis, P.; Spek, A. L. Bypass - an effective method for the refinement of crystal-structures containing disordered solvent regions. *Acta Crystallogr., Sect. A* **1990**, *46*, 194-201.
5. (a) Segall, M.; Linda, P.; Probert, M.; Pickard, C.; Hasnip, P.; Clark, S.; Payne, M. Materials Studio CASTEP Version 2.2 (2002). (b) Adamo, C.; Barone, V. Physically motivated density functionals with improved performances: The modified Perdew-Burke-Ernzerhof model. *J. Chem. Phys.* **2002**, *116*, 5933-5940.
6. Perdew, J. P.; Burke, K.; Ernzerhof, M. Generalized gradient approximation made simple. *Phys. Rev. Lett.* **1996**, *77*, 3865-3868.
7. Hamann, D. R.; Schlüter, M.; Chiang, C. Norm-conserving pseudopotentials. *Phys. Rev. Lett.* **1979**, *43*, 1494-1497.
8. Ohno, Y. Color rendering and luminous efficacy of white LED spectra. *Proc. SPIE* **2004**, 5530, 88-98.